

# Performance Analysis of Fluid Antenna Multiple Access Assisted Wireless Powered Communication Network

Xiao Lin, Yizhe Zhao, *Member, IEEE*, Halvin Yang, and Jie Hu, *Senior Member, IEEE*

**Abstract**—This paper investigates a novel fluid antenna multiple access (FAMA)-assisted wireless powered communication network (WPCN), in which a hybrid access point (HAP) equipped with multiple fixed position antennas (FPAs) provides integrated data and energy transfer (IDET) services towards low-power devices that are equipped with a single fluid antenna (FA), while the low-power devices use harvested energy to power their own uplink transmission. Using the block correlation channel model, both the downlink and uplink wireless data transfer (WDT) outage probabilities are analyzed under specific port selection strategies, including downlink signal-to-interference ratio-based port selection (DSPS) strategy, downlink energy harvesting power-based port selection (DEPS) strategy, uplink signal-to-noise ratio-based port selection (USPS) strategy, and uplink channel-based port selection (UCPS) strategy. A step function approximation (SFA) approach is also relied upon to derive closed-form expressions for the outage probabilities, while the lower bounds for uplink WDT outage probabilities are also formulated. Numerical results demonstrate the validity of our theoretical analysis, which also provide useful guidelines for the system design through the analytical framework.

**Index Terms**—Fluid antenna multiple access (FAMA), wireless powered communication network (WPCN), port selection strategy, outage probability.

## I. INTRODUCTION

### A. Background

Recently, the rapid advancement of wireless mobile communications has improved significantly, leading to the emergence of multiple progressive technologies, *i.e.*, multiple-input-multiple-output (MIMO), which increased the capacity and the efficiency of the network. However, most of the connected devices are tiny and energy-limited, which have both communication and energy replenishment requirements. Since it is cost-prohibitive and impractical to replace the batteries of these devices manually in some challenging environments, wireless energy transfer (WET) has emerged as a promising technology to extend the battery lifespan of such devices. By coordinating with wireless data transfer (WDT), the receiver is able to perform energy harvesting (EH) and information decoding (ID) simultaneously, which yields the concept of integrated data and energy transfer (IDET) [1], [2]. Further, wireless powered communication network (WPCN) is studied as a typical paradigm for serving all the low-power devices,

which is capable of gleaning radio frequency (RF) energy for powering their own uplink transmission. With the aid of the technique of WET or IDET, the problem of energy limitations of wireless devices can be readily alleviated [3], [4].

However, due to the limitation of the energy harvesting circuit, WET has a higher requirement on the receive signal strength compared to WDT, which is posing a challenge on the efficiency of wireless signals' transmission. Although the MIMO technology has significantly boomed wireless mobile communications, it is not suitable for small low-power devices due to its higher power consumption and increased hardware complexity. To overcome this bottleneck, fluid antenna (FA) systems have emerged as a viable technology. Unlike traditional MIMO, which requires multiple fixed antennas separated by sufficient distances to achieve spatial diversity, FA is able to achieve comparable diversity within a tiny space by flexibly adjusting the antenna shape and position [5]. This characteristic is particularly advantageous for IDET in WPCN due to its ability to enhance the WDT and WET.

The FA system can also be applied in the multi-user scenario, which yields the concept of fluid antenna multiple access (FAMA) [6], [7]. With the aid of FAMA, it is able to mitigate the interference and enhance the signal-to-interference-plus-noise ratio (SINR) by selecting the optimal port where the signal envelopes from the other users were in a deep fade. However, as for the multi-user FAMA-assisted WPCN system, the port selection strategies should be quite different, since the interference at the receiver plays a different role for WET and WDT, *i.e.*, the interference may negatively impact the information decoding, but can boost the energy harvesting performance. In order to unveil the trade-off between WET and WDT, this paper will focus on the multi-user scenario and investigate the performance analysis of the FAMA-assisted WPCN.

### B. Related Works

Due to the hardware limitations, one of the challenges in designing IDET systems is that ID and EH cannot be implemented through the same circuit module. Therefore, time switching (TS) and power splitting (PS) are two basic approaches to address this issue [8]. In the TS approach, the received signal is periodically directed for ID and EH via a time switcher, while in the PS approach, the signal received at the receiver is separated into two parts, one for ID and the other for EH. IDET has been widely studied in various scenarios. For instance, the ergodic throughput in fading relay channels was investigated with IDET in [9], an adaptive power

Xiao Lin, Yizhe Zhao and Jie Hu are with the School of Information and Communication Engineering, University of Electronic Science and Technology of China, Chengdu 611731, China. (e-mail: xiaolin@std.uestc.edu.cn; yzzhao@uestc.edu.cn; hujie@uestc.edu.cn).

Halvin Yang is with the Wolfson School of Mechanical, Electrical and Manufacturing Engineering, Loughborough University, Loughborough, LE11 3TU, United Kingdom. (e-mail: h.yang6@lboro.ac.uk).

allocation scheme for IDET-enabled full-duplex cooperative non-orthogonal multiple access (NOMA) networks using a time-switching protocol was investigated in [10]. Also, IDET was studied in the MIMO interference channel [11]. On the other hand, WPCN has also attracted significant attention, *e.g.*, Budhiraja *et al.* [12] maximized the energy efficiency for wireless powered based D2D communication systems, and Ju *et al.* [13] proposed a novel common-throughput maximization approach for WPCN. Moreover, some other technologies, *e.g.*, MIMO [14], unmanned aerial vehicle (UAV) [15], and reconfigurable intelligent surface (RIS) [16] were also studied in the WPCN in order to enhance both the WDT and WET performance. Besides, relay selection has also been considered in the WPCN, since it may directly influence the WDT and WET performance by coordinating different wireless channels. For instance, in [17], the asymptotic distribution of the throughput of the  $k$ -th best link over fading channels was derived using extreme value theory. In [18], the system outage probability and reliable throughput were derived based on the joint optimal selection of the  $k$ -th best relay and the transmit antenna.

On the other hand, in order to improve the efficiency of wireless signals' transmission, FA has been considered in various wireless communication scenarios. Specifically, New *et al.* in [19] approximated the outage probability and diversity gain of the FA system in closed-form expressions into the single-input and single-output (SISO) system, while the achievable performance of the FA system-assisted MIMO systems was further studied in [20]. Moreover, FAMA systems were also studied in [21], [22] to improve the spectrum efficiency of the system without utilizing additional communication resources. For instance, Wong *et al.* studied the benefits of the synergy between opportunistic scheduling and FAMA [21], and Xu *et al.* investigated the outage performance of a downlink FAMA system having two users under a fully correlated channel model [22].

The FA system has also been investigated by integrating the technology of IDET [23], [24], [25], [26], [27], [28] in WPCN. These studies have provided significant insights into the potential of FA in WET scenarios. Specifically, the WDT as well as WET performance of the FA-assisted IDET system were evaluated theoretically by conceiving the TS approach [23] and PS approach [24], [25]. Moreover, Zhang *et al.* optimized the weighted energy harvesting power of energy receivers by satisfying the SINR constraints for each data receiver, which are all equipped with a single FA [26]. Lai *et al.* first derived the analytical outage probability of the one-dimensional (1D) FA-assisted wireless powered communication system [27], while Ghadi *et al.* studied the performance of the 2D FA-assisted WPCN under the NOMA scheme [28].

### C. Motivations and Contributions

Despite the advantages in both WET and FA technologies, the study of FA in the WPCN remains uncharted territory, presenting several challenges: 1) The spatial correlation between FA ports complicates the derivation of outage probability, making performance analysis of the WPCN difficult; 2) The complex expression of outage probability hinders the provision

of insights into future FA system design; 3) Since the port selection strategy in FA can be tailored to different requirements, its impact on downlink and uplink WDT performance in WPCN remains unclear; 4) The interference of the FAMA-assisted multi-user scenario has different impacts on the WDT and WET performance, which should be further investigated.

In order to address these challenges, this paper aims to study the outage probability analysis of FAMA-assisted WPCN with a more practical wireless channel model by considering various port selection strategies. Specifically, in the considered system, a hybrid access point (HAP) with multiple traditional antennas communicates with multi-users equipped with a single FA. The PS approach is conceived at the receiver to simultaneously coordinate WDT and WET for realizing downlink IDET, while the receivers also use gleaned energy for powering their uplink transmission. Although the multi-user interference may degrade WDT performance, it can provide additional RF sources for EH to further boost the uplink transmission. Our main contributions of this paper are then summarized as follows:

- We study an FAMA-assisted WPCN system, while the outage performance is analyzed theoretically under some typical port selection strategies, including: 1) downlink signal-interference-ratio based port selection (DSPS) strategy; 2) downlink energy harvesting power based port selection (DEPS) strategy; 3) uplink channel based port selection (UCPS) strategy; and 4) uplink signal-to-noise ratio based port selection (USPS) strategy.
- The closed-forms of the downlink WDT outage probabilities are obtained under the USPS, DEPS, and UCPS strategies, while an exact expression of that under the DSPS strategy is also formulated. For the uplink WDT outage probabilities, we derive exact expressions under the USPS, DEPS, and UCPS strategies, while an approximate closed-form solution for the DSPS strategy is obtained.
- The step function approximation (SFA) is relied upon to derive more computationally efficient closed-form expressions under the DSPS strategy, while some more analytically tractable closed-form expressions under the USPS, DEPS, and UCPS strategies are also obtained. Furthermore, the lower bounds of outage probabilities for these strategies are also derived for providing valuable insights for system design.
- Numerical results validate our analytical findings and demonstrate the effectiveness of our approximate method.

The rest of this paper is organized as follows. In Section II, we introduce the FAMA-assisted WPCN system and discuss the block correlation channel model. Section III provides the analysis of downlink WDT outage probabilities and uplink WDT outage probabilities by considering different port selection strategies. The theoretical analysis is validated in Section IV, and finally, Section V concludes the paper.

## II. SYSTEM MODEL

We consider a FAMA-assisted WPCN system consisting of an HAP and  $M$  users, where the HAP is equipped with

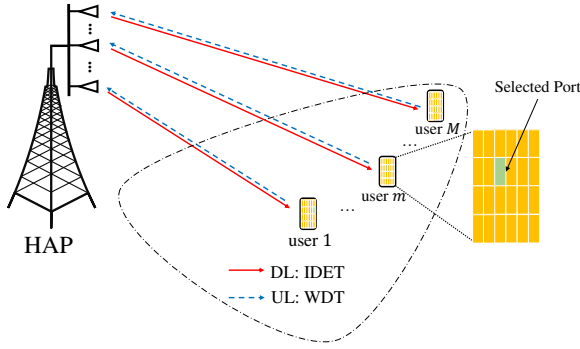


Fig. 1. A system of FAMA-assisted WPCN.

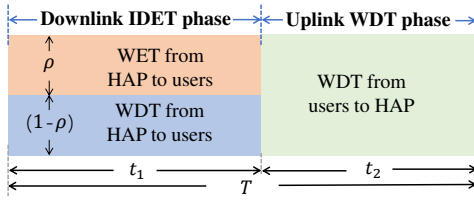


Fig. 2. A transmission framework of the FAMA-assisted WPCN system.

$M$  fix-position antennas (FPAs) and each user is equipped with a single FA having  $N$  ports<sup>1</sup>. Each HAP antenna serves a corresponding user for WDT, *i.e.*, the  $m$ -th HAP antenna communicates with user  $m$ . The timeline is divided into several periods, each lasting  $T$ . At the beginning of each period, the user activates one port based on a specific port selection strategy<sup>2</sup>, and it remains unchanged throughout the period for the execution of downlink IDET and uplink WDT. Then, during the downlink IDET phase<sup>3</sup> having the duration of  $t_1$ ,  $0 < t_1 < T$ , the HAP transmits dedicated RF signals towards all the users via their corresponding antennas, while each user applies the PS approach for realizing downlink IDET. Subsequently, during the uplink WDT phase having the duration of  $t_2$  ( $t_2 = T - t_1$ ), each user uploads information to the HAP by using all the harvested energy via the same port. Note that since the HAP is equipped with traditional antennas, it is unable to coordinate multi-user interference via FAMA. Therefore, in the uplink phase, all the users upload their own information using orthogonal resources to avoid any interference at the HAP. Without loss of generality, the following analysis concerns the typical user  $m$  but the results hold for all the users of the proposed system.

### A. Signal Model

In the downlink IDET phase, user  $m$  employs the PS approach to coordinate WDT and WET from the received signal. Specifically, the received signal at each UE is split by a power splitter which divides  $\rho^{(m)}$  ( $0 \leq \rho^{(m)} \leq 1$ ) portion

<sup>1</sup>The FA structure can be a linear (1D) or planar (2D) FA based on radio frequency (RF) pixels.

<sup>2</sup>Given that an RF-based pixel FA is considered, it is reasonable to assume that the energy consumed during port switching is negligible.

<sup>3</sup>This paper considers an RF pixel-based FA, thus, it is reasonably assumed that the time for port selection is negligible.

of the signal power for WDT, and the remaining  $(1 - \rho^{(m)})$  portion of power for WET. Therefore, the received WDT signal at the  $n$ -th port FA of user  $m$  is

$$r_{D,n}^{(m)} = s_D^{(m)} \sqrt{\frac{\rho^{(m)} P_D^{(m,m)}}{\Omega}} g_n^{(m,m)} + \sum_{\substack{\tilde{m}=1 \\ \tilde{m} \neq m}}^M s_D^{(\tilde{m})} \sqrt{\frac{\rho^{(\tilde{m})} P_D^{(\tilde{m},m)}}{\Omega}} g_n^{(\tilde{m},m)} + w_{D,n}^{(m)}, \quad (1)$$

where  $s_D^{(m)} \in \mathbb{C}$  is the downlink signal intended for user  $m$  having the unit power, *i.e.*,  $\mathbb{E}[|s_D^{(m)}|^2] = 1$ ,  $P_D^{(\tilde{m},m)}$  is the transmit power of  $\tilde{m}$ -th HAP antenna and is assumed to be the same as  $P_t$  for each transmit antenna without loss of generality,  $g_n^{(\tilde{m},m)} \forall n \in \mathcal{N}$  is the channel coefficient from the  $\tilde{m}$ -th HAP antenna to the  $n$ -th port of user  $m$ 's FA,  $w_{D,n}^{(m)} \sim \mathcal{CN}(0, \sigma_w^2)$  is the additive white Gaussian noise (AWGN) at the FA of user  $m$ ,  $\Omega$  is the path loss<sup>4</sup>. Then, by applying the PS approach, the energy harvesting power (EHP) at the  $n$ -th port of user  $m$  is expressed by

$$E_n^{(m)} = (1 - \rho^{(m)}) \frac{P_t t_1}{\Omega} \sum_{\tilde{m}=1}^M |g_n^{(\tilde{m},m)}|^2. \quad (2)$$

Accordingly, by neglecting the noise item, the received signal-to-interference ratio (SIR)<sup>5</sup> at the  $n$ -th port of user  $m$  is given by

$$\gamma_{D,n}^{(m)} = \frac{|g_n^{(m,m)}|^2}{\sum_{\substack{\tilde{m}=1 \\ \tilde{m} \neq m}}^M |g_n^{(\tilde{m},m)}|^2}. \quad (3)$$

During the uplink WDT phase, the received signal at the HAP from the  $n$ -th port of the typical user  $m$  is expressed as

$$r_{U,n}^{(m)} = s_U^{(m)} \sqrt{\frac{P_n^{(m)}}{\Omega}} h_n^{(m)} + w_U^{(m)}, \quad (4)$$

where  $P_n^{(m)} = \frac{E_n^{(m)}}{t_2}$  is the transmission power available for the uplink WDT phase.  $h_n^{(m)}$  is the uplink multi-path fading coefficient from the  $n$ -th fluid antenna port of the user  $m$  to the corresponding antenna of the HAP.  $s_U^{(m)}$  is the uplink information signal with  $\mathbb{E}[|s_U^{(m)}|^2] = 1$ , and  $w_U^{(m)} \sim \mathcal{CN}(0, \sigma_w^2)$  is the AWGN at the HAP antenna. Since there is no additional interference during the uplink transmission, the signal-to-noise ratio (SNR) at the HAP for receiving the user  $m$ 's uplink signal is given as

$$\gamma_{U,n}^{(m)} = \frac{|h_n^{(m)}|^2}{t_2 \sigma_w^2 \Omega} E_n^{(m)}. \quad (5)$$

<sup>4</sup>Without loss of generality, it is assumed that the pathloss between the HAP and different users remains the same.

<sup>5</sup>In this paper, we assume that the system is operating in an interference-limited scenario. Thus, the interference power is much greater than the noise power, and SIR serves as a suitable approximation for the SINR.

## B. Wireless Channel Model

The spatial separation among the ports of FA yields a difference in the phases of arriving paths, thus inducing correlation between the channels following Jake's model between the  $n_1$ -th port and the  $n_2$ -th port, which is modeled as [29]

$$(\Sigma)_{n_1, n_2} = J_0 \left( \frac{2\pi(n_1 - n_2)W}{N - 1} \right), n_1, n_2 \in \mathcal{N}, \quad (6)$$

where  $J_0(\cdot)$  is the zero-order Bessel function of the first kind. Although the model can accurately characterize the correlation, it makes the analysis challenging to conduct. To address this issue, [30] proposed the block-correlation model to simplify the representation of (6). In this model, different blocks are defined to be independent, while the spatial correlation within each block remains constant. The spatial correlation over the ports is characterized as

$$\widehat{\Sigma} \in \mathbb{R}^{N \times N} = \begin{pmatrix} \mathbf{A}_1 & \mathbf{0} & \dots & \mathbf{0} \\ \mathbf{0} & \mathbf{A}_2 & \dots & \mathbf{0} \\ \vdots & & \ddots & \vdots \\ \mathbf{0} & \mathbf{0} & \mathbf{0} & \mathbf{A}_B \end{pmatrix}, \quad (7)$$

where each submatrix  $\mathbf{A}_b$  is a constant correlation matrix having the size of  $L_b$  and correlation of  $\mu^2$ , which is given by

$$\mathbf{A}_b \in \mathbb{R}^{L_b \times L_b} = \begin{pmatrix} 1 & \mu^2 & \dots & \mu^2 \\ \mu^2 & 1 & \dots & \mu^2 \\ \vdots & & \ddots & \vdots \\ \mu^2 & \dots & \mu^2 & 1 \end{pmatrix}, \quad b = 1, \dots, B. \quad (8)$$

where  $\mu^2$  is a constant close to 1,  $\sum_{b=1}^B L_b = N$ . The block sizes  $L_b$  and block number  $B$  are chosen based on spectral analysis of the true correlation matrix in (6), and the detailed information can be found in [30]. Thus, the wireless channel between the  $m$ -th antenna at HAP and the user  $m$  in the downlink IDET phase can be re-expressed as<sup>6</sup>

$$g_{n,b(n)}^{(m,m)} = \sqrt{1 - \mu^2} x_{n,b(n)}^{(m,m,D)} + \mu x_{b(n)}^{(m,m,D)} + j \left( \sqrt{1 - \mu^2} y_{n,b(n)}^{(m,m,D)} + \mu y_{b(n)}^{(m,m,D)} \right), \quad (9)$$

and the wireless channel between the user  $m$  and the HAP in the uplink WDT phase can be re-expressed as

$$h_{n,b(n)}^{(m)} = \sqrt{1 - \mu^2} x_{n,b(n)}^{(m,U)} + \mu x_{b(n)}^{(m,U)} + j \left( \sqrt{1 - \mu^2} y_{n,b(n)}^{(m,U)} + \mu y_{b(n)}^{(m,U)} \right), \quad (10)$$

where  $x_{n,b(n)}^s, x_{b(n)}^s, y_{n,b(n)}^s, y_{b(n)}^s, s \in \{(m, m, D), (m, U)\}$  are all independent Gaussian variables with zero mean and variance of 1.  $b(n)$  is the block index, *i.e.*,  $b(n) = 1$  for  $n = 1, \dots, L_1$ ,  $b(n) = 2$  for  $n = L_1 + 1, \dots, L_1 + L_2$ , and so on [30]. For simplicity of notation, we use  $n$  to represent  $n, b(n)$  in the following, *e.g.*,  $x_n^{(m)}$  represents  $x_{n,b(n)}^{(m)}$ . In this paper, the outage performance of the FAMA-assisted WPCN system will be analyzed based on the block-correlation model described above.

<sup>6</sup>In this paper, we assume that the system is operating in a rich scattering environment.

## III. OUTAGE PROBABILITY ANALYSIS

The performance of the proposed FAMA-assisted WPCN is analyzed in terms of the WDT outage probability for both the downlink and uplink phases. A downlink WDT outage occurs when the received SIR at a typical user  $m$  falls below a certain threshold, which is defined as

$$P(\gamma_{\text{th}}^{\text{D}}) = \Pr \left( \gamma_{\text{D}, n^*}^{(m)} = \frac{|g_{n^*}^{(m,m)}|^2}{\sum_{\substack{\bar{m}=1 \\ \bar{m} \neq m}}^M |g_{n^*}^{(\bar{m},m)}|^2} < \gamma_{\text{th}}^{\text{D}} \right), \quad (11)$$

where  $n^*$  is the selected port determined by the specific port selection strategies and  $\gamma_{\text{th}}^{\text{D}}$  is the minimum required SIR threshold for WDT in the downlink IDET phase. Similarly, an uplink WDT outage occurs when the received SNR at the HAP is below a certain threshold, which is defined as

$$P(\gamma_{\text{th}}^{\text{U}}) = \Pr \left( \gamma_{\text{U}, n^*}^{(m)} = \frac{|h_{n^*}^{(m)}|^2}{t_2 \sigma_w^2 \Omega} E_{n^*}^{(m)} < \gamma_{\text{th}}^{\text{U}} \right), \quad (12)$$

where  $\gamma_{\text{th}}^{\text{U}}$  is the minimum required SNR threshold in the uplink WDT.

### A. Port Selection Strategies

In each period, the transmission process consists of two phases: downlink IDET and uplink WDT. A natural approach is to explore different port selection strategies to optimize either the downlink WDT performance or the uplink WDT performance. Specifically, to improve the the downlink WDT performance, the port selection can be adjusted to maximize the received SIR, which yields the downlink SIR-based port selection (DSPS) strategy. To improve the uplink WDT outage performance, the port selection can be adjusted to maximize the receive SNR at the HAP, which yields the uplink SNR based port selection (USPS) strategy. Note that the received SNR at the HAP depends on both the downlink energy harvesting power during the downlink IDET phase and the uplink channel, which indicates that if the USPS strategy is adopted, the receiver should be aware of both the uplink and downlink channel among all the ports. Unfortunately, this may bring inevitable complexity and power consumption, which is not friendly to the low-power devices. Therefore, it is rational to simplify the USPS strategy into two sub-ones, namely downlink energy harvesting power based port selection (DEPS) strategy and uplink channel based port selection (UCPS) strategy. Note that by adopting either the DEPS or the UCPS strategy, only the single-side channel state information is required, which reduces the port selection complexity. However, due to the non-global information, the DEPS and UCPS strategy would perform worse than the USPS strategy on the uplink WDT performance. Therefore, this work aims to analyze downlink and uplink WDT outage performance based on these four port selection strategies.

### B. Outage Probabilities under the DSPS Strategy

In the DSPS strategy, the user selects the port having the highest SIR, without considering the uplink channel. When the

$$\begin{aligned}
 G(\gamma_{\text{th}}^{\text{D}}; r_b, \tilde{r}_b) &= Q_{M-1} \left( \sqrt{\frac{\mu^2 \gamma_{\text{th}}^{\text{D}} \tilde{r}_b}{(1-\mu^2)(\gamma_{\text{th}}^{\text{D}}+1)}}, \sqrt{\frac{\mu^2 r_b}{(1-\mu^2)(\gamma_{\text{th}}^{\text{D}}+1)}} \right) - \left( \frac{1}{\gamma_{\text{th}}^{\text{D}}+1} \right)^{M-1} \exp \left( -\frac{\mu^2}{2(1-\mu^2)} \frac{\gamma_{\text{th}}^{\text{D}} \tilde{r}_b + r_b}{\gamma_{\text{th}}^{\text{D}}+1} \right) \\
 &\quad \times \sum_{l=0}^{M-2} \sum_{j=0}^{M-l-2} \frac{(M-(j+l)-1)_j}{j!} \left( \frac{r_b}{\tilde{r}_b} \right)^{\frac{j+l}{2}} (\gamma_{\text{th}}^{\text{D}}+1)^l (\gamma_{\text{th}}^{\text{D}})^{\frac{j-l}{2}} I_{j+l} \left( \frac{\mu^2 \sqrt{\gamma_{\text{th}}^{\text{D}} r_b \tilde{r}_b}}{(1-\mu^2)(\gamma_{\text{th}}^{\text{D}}+1)} \right) \quad (18)
 \end{aligned}$$

user  $m$  applies the DSPS strategy, the optimal antenna port  $n^*$  is selected to maximize the  $\gamma_{\text{D},n}^{(m)}$  as

$$n^* = \arg \max_n \frac{|g_n^{(m,m)}|^2}{\sum_{\tilde{m} \neq m}^M |g_n^{(\tilde{m},m)}|^2} = \arg \max_n \frac{X_n}{Y_n}. \quad (13)$$

where  $X_n$  and  $Y_n$  are defined as

$$\begin{aligned}
 X_n &= \left( x_n^{(m,m,\text{D})} + \frac{\mu x_{b(n)}^{(m,m,\text{D})}}{\sqrt{1-\mu^2}} \right)^2 \\
 &\quad + \left( y_n^{(m,m,\text{D})} + \frac{\mu y_{b(n)}^{(m,m,\text{D})}}{\sqrt{1-\mu^2}} \right)^2, \quad (14)
 \end{aligned}$$

$$\begin{aligned}
 Y_n &= \sum_{\substack{\tilde{m} \neq m \\ \tilde{m}=1}}^M \left( x_n^{(\tilde{m},m,\text{D})} + \frac{\mu x_{b(n)}^{(\tilde{m},m,\text{D})}}{\sqrt{1-\mu^2}} \right)^2 \\
 &\quad + \left( y_n^{(\tilde{m},m,\text{D})} + \frac{\mu y_{b(n)}^{(\tilde{m},m,\text{D})}}{\sqrt{1-\mu^2}} \right)^2. \quad (15)
 \end{aligned}$$

Thus, the downlink WDT outage probability is expressed as

$$P_{\text{DSPA}}^{\text{D}}(\gamma_{\text{th}}^{\text{D}}) = \Pr \left( \arg \max_n \frac{X_n}{Y_n} < \gamma_{\text{th}}^{\text{D}} \right). \quad (16)$$

*Theorem 1:* By applying the DSPS strategy, the downlink WDT outage probability is formulated as

$$\begin{aligned}
 P_{\text{DSPA}}^{\text{D}}(\gamma_{\text{th}}^{\text{D}}) &= \prod_{b=1}^B \int_0^\infty \int_0^\infty \frac{\tilde{r}_b^{M-2} e^{-r_b - \tilde{r}_b}}{\Gamma(M-1)} \times \\
 &\quad [G(\gamma_{\text{th}}^{\text{D}}; 2r_b, 2\tilde{r}_b)]^{L_b} dr_b d\tilde{r}_b, \quad (17)
 \end{aligned}$$

where  $G(\gamma; r_b, \tilde{r}_b)$  is provided as in Eq. (18),  $\Gamma(\cdot)$  is the Gamma function,  $Q_p(\cdot)$  is the  $p$ -th order Marcum Q-function, and  $I_p(\cdot)$  is the  $p$ -th order modified Bessel function of the first kind.

*Proof:* The proof of this result can be found in [30, Appendix B]. ■

In order to provide a more concise result on the downlink WDT outage probability, we first introduce the SFA as follows.

*Lemma 1:* Marcum-Q function can be approximated by a step function as

$$Q_p(a, b) = \begin{cases} 0, & a < b \\ 1, & a > b \end{cases} \quad (19)$$

*Proof:* In [30, Corollary 3], it has been demonstrated that  $Q_p(a, b)$  can be approximated by the Heaviside step function

shifted at a threshold, *i.e.*, a relatively small neighborhood around  $a$ . Note that when  $a < b$  and  $b \rightarrow \infty$ , we have  $Q_p(a, b) \rightarrow 0$ . When  $a > b$  and  $a \rightarrow \infty$ , we have  $Q_p(a, b) \rightarrow 1$ . Based on this fact, the SFA is then proposed as in Eq. (19). ■

*Corollary 1:* By using the SFA, the downlink WDT outage probability under the DSPS strategy is approximated by

$$\begin{aligned}
 P_{\text{DSPA}}^{\text{D}}(\gamma_{\text{th}}^{\text{D}}) &= \prod_{b=1}^B \int_0^\infty \int_0^\infty \frac{\tilde{r}_b^{M-2} e^{-r_b - \tilde{r}_b}}{\Gamma(M-1)} \\
 &\quad \times [\tilde{G}(\gamma_{\text{th}}^{\text{D}}; r_b, \tilde{r}_b)]^{L_b} dr_b d\tilde{r}_b. \quad (20)
 \end{aligned}$$

where  $\tilde{G}(\gamma_{\text{th}}^{\text{D}}; r_b, \tilde{r}_b) = Q_{M-1} \left( \sqrt{\frac{2\mu^2 \tilde{r}_b}{1-\mu^2}}, \sqrt{\frac{2\mu^2 r_b}{(1-\mu^2)\gamma_{\text{th}}^{\text{D}}}} \right)$ .

*Proof:* Please refer to Appendix A for the detailed proof. ■

*Corollary 2:* The downlink WDT outage probability by applying the DSPS strategy can further be approximated as

$$P_{\text{DSPA}}^{\text{D}}(\gamma_{\text{th}}^{\text{D}}) \approx \left[ 1 - \frac{1}{(1 + \gamma_{\text{th}}^{\text{D}})^{M-1}} \right]^B. \quad (21)$$

*Proof:* By applying the SFA to Eq. (20) once again, it can be approximated as

$$P_{\text{DSPA}}^{\text{D}}(\gamma_{\text{th}}^{\text{D}}) \approx \prod_{b=1}^B \int_0^\infty \int_0^\infty \frac{\tilde{r}_b^{M-2} e^{-r_b - \tilde{r}_b}}{\Gamma(M-1)} \int_0^{\gamma_{\text{th}}^{\text{D}} \tilde{r}_b} e^{-r_b} dr_b d\tilde{r}_b. \quad (22)$$

Then, with the aid of Eq. (3.381.4) in [31], Eq. (21) is further derived, which completes the proof. ■

After that, we will work on the uplink WDT outage probability under the DSPS strategy as

$$\begin{aligned}
 P_{\text{DSPA}}^{\text{U}}(\gamma_{\text{th}}^{\text{U}}) &= \Pr \left( \gamma_{\text{U},n^*}^{(m)} < \gamma_{\text{th}}^{\text{U}} | n^* = \arg \max_n \gamma_{\text{D},n}^{(m)} \right) \\
 &= \Pr \left( \beta_{n^*} \alpha_{n^*} < \tilde{\gamma} | n^* = \arg \max_n \frac{X_n}{Y_n} \right), \quad (23)
 \end{aligned}$$

where  $\tilde{\gamma} = \frac{\gamma_{\text{th}}^{\text{U}} t_2 \sigma_w^2 \Omega^2}{(1-\rho^{(m)}) P_t t_1 (1-\mu^2)^2}$ ,  $\alpha_n = X_n + Y_n$ , and the variable  $\beta_n$  is defined as

$$\beta_n = \left( x_n^{(m,\text{U})} + \frac{\mu x_{b(n)}^{(m,\text{U})}}{\sqrt{1-\mu^2}} \right)^2 + \left( y_n^{(m,\text{U})} + \frac{\mu y_{b(n)}^{(m,\text{U})}}{\sqrt{1-\mu^2}} \right)^2. \quad (24)$$

In order to evaluate the uplink WDT outage probability, we first introduce the following Lemma as

*Lemma 2:* When  $\mu^2 = 1$ , the variables  $\frac{X_n}{Y_n}$  and  $X_n + Y_n$  are independent.

*Proof:* Please refer to Appendix B for the detailed proof. ■

*Theorem 2:* The uplink WDT outage probability under the DSPS strategy can be approximated as

$$P_{\text{DSPS}}^{\text{U}}(\gamma_{\text{th}}^{\text{U}}) \approx 1 - \frac{[\tilde{\gamma}(1 - \mu^2)]^{\frac{M}{2}}}{2^{M-1}\Gamma(M)} K_M\left(\sqrt{\tilde{\gamma}(1 - \mu^2)}\right), \quad (25)$$

where  $K_p(\cdot)$  is the  $p$ -th modified Bessel function of the second kind.

*Proof:* Please refer to Appendix C for the detailed proof. ■

*Remark 1:* The uplink WDT outage probability under the DSPS strategy is independent of  $N$  and  $W$ , while the multi-port FA can be degenerated to a single antenna.

*Corollary 3:* As  $\gamma_{\text{th}}^{\text{U}}$  increases or  $P_t$  decreases, the uplink WDT outage probability  $P_{\text{DSPS}}^{\text{U}}$  increases.

*Proof:* Due to the fact that

$$\frac{\partial(z^v K_v(z))}{\partial z} = -z^v K_{v-1}(z) < 0, \quad (26)$$

$P_{\text{DSPS}}^{\text{U}}(\gamma_{\text{th}}^{\text{U}})$  monotonously decreases as  $\tilde{\gamma}$  increases. Besides, since we have  $\tilde{\gamma} = \frac{\gamma_{\text{th}}^{\text{U}} t_2 \sigma_w^2 \Omega^2}{(1 - \rho^{(m)}) P_t t_1 (1 - \mu^2)^2}$ , it increases when we increase  $\gamma_{\text{th}}^{\text{U}}$  or decrease  $P_t$ , which further completes the proof. ■

### C. Outage Probabilities under the DEPS Strategy

In this section, we will analyze the outage performance under the DEPS strategy. In the DEPS strategy, the user adjusts the port based on the EHP at user  $m$ . In other words, the DEPS strategy selects the port that harvests the maximum amount of energy. If the user applies the DEPS strategy, the optimal antenna port  $n^*$  is selected by following

$$n^* = \arg \max_n E_n^{(m)} = \arg \max_n \sum_{\tilde{m}=1}^M \left| g_n^{(\tilde{m}, m)} \right|^2. \quad (27)$$

Then, our first objective is to analyze the downlink WDT outage probability, which is expressed as

$$\begin{aligned} P_{\text{DEPS}}^{\text{D}}(\gamma_{\text{th}}^{\text{D}}) &= \Pr\left(\gamma_{\text{D}, n^*}^{(m)} < \gamma_{\text{th}}^{\text{D}} | n^* = \arg \max_n E_n^{(m)}\right), \\ &= \Pr\left(\frac{X_{n^*}}{Y_{n^*}} < \gamma_{\text{th}}^{\text{D}} | n^* = \arg \max_n (X_n + Y_n)\right). \end{aligned} \quad (28)$$

Then, with the aid of the transformation of  $P_{\text{DEPS}}^{\text{D}}$ , an approximation of the WDT outage probability can be obtained by the following theorem.

*Theorem 3:* The downlink WDT outage probability under the DEPS strategy can be approximated as

$$P_{\text{DEPS}}^{\text{D}}(\gamma_{\text{th}}^{\text{D}}) \approx 1 - \frac{1}{(\gamma_{\text{th}}^{\text{D}} + 1)^{M-1}}. \quad (29)$$

*Proof:* Please refer to Appendix D for the detailed proof. ■

Next, we will work out the uplink WDT outage probability under the DEPS strategy, which is expressed as

$$\begin{aligned} P_{\text{DEPS}}^{\text{U}}(\gamma_{\text{th}}^{\text{U}}) &= \Pr\left(\gamma_{\text{U}, n^*}^{(m)} < \gamma_{\text{th}}^{\text{U}} | n^* = \arg \max_n E_n^{(m)}\right) \\ &= \Pr\left(\alpha_n^* \beta_{n^*} < \tilde{\gamma} | n^* = \arg \max_n \alpha_n\right) \quad (30) \\ &\stackrel{(a)}{=} \Pr\left(\max_n \alpha_n < \frac{\tilde{\gamma}}{\beta_{n^*}}\right), \end{aligned}$$

where (a) accounts for the fact that  $\alpha_n$  is independent of  $\beta_{n^*}$ . Then, the uplink WDT outage probability is analyzed in the following theorem.

*Theorem 4:* The uplink WDT outage probability under the DEPS strategy is formulated as in Eq. (31).

*Proof:* Please refer to Appendix E for the detailed proof. ■

*Corollary 4:* The uplink WDT outage probability under the DEPS strategy is further approximated by

$$P_{\text{DEPS}}^{\text{U}}(\gamma_{\text{th}}^{\text{U}}) \approx \int_0^\infty e^{-x} \left[ \frac{\Phi\left(M, \frac{\gamma_{\text{th}}^{\text{U}} t_2 \sigma_w^2 \Omega^2}{4\mu^2(1-\rho^{(m)})P_t t_1 x}\right)}{\Gamma(M)} \right]^B dx. \quad (32)$$

where  $\Phi(a, x) = \int_0^x t^{a-1} e^{-t} dt$  is the lower incomplete gamma function.

*Proof:* By applying the SFA, Eq. (31) can be simplified as

$$\begin{aligned} P_{\text{DEPS}}^{\text{D}}(\tilde{\gamma}) &= \int_{x=0}^\infty (1 - \mu^2) \exp[-(1 - \mu^2)x] \\ &\quad \times \prod_{b=1}^B \int_{r_b=0}^{\frac{\tilde{\gamma}(1-\mu^2)}{4\mu^2 x}} \frac{(r_b)^{M-1} \exp(-r_b)}{\Gamma(M)} dr_b. \end{aligned} \quad (33)$$

Then, with the aid of Eq. (3.351.1) in [31], Eq. (32) is obtained with some further simplifications, which completes the proof. ■

*Proposition 1:* The uplink WDT outage probability under the DEPS strategy is lower bounded by

$$P_{\text{DEPS}}^{\text{U}}(\tilde{\gamma}) > \int_0^\infty e^{-x} \left[ \frac{\Phi\left(M, \frac{\hat{\gamma}}{x}\right)}{\Gamma(M)} \right]^B dx, \quad (34)$$

where  $\hat{\gamma} = \frac{\gamma_{\text{th}}^{\text{U}} t_2 \sigma_w^2 \Omega^2}{4(1-\rho^{(m)})P_t t_1}$ .

*Proof:* Please refer to Appendix F for the detailed proof. ■

*Proposition 2:* The uplink WDT outage probability under the DEPS strategy is further lower bounded by

$$P_{\text{DEPS}}^{\text{U}}(\hat{\gamma}) > \sum_{b=0}^{BM} (-1)^b \sqrt{b\hat{\gamma}d_M} K_1\left(\sqrt{b\hat{\gamma}d_M}\right), \quad (35)$$

where  $d_M = [\Gamma(1 + M)]^{-1/M}$ .

*Proof:* According to [32], the lower bound for the incomplete gamma function is provided as

$$\frac{\Phi(a, x)}{\Gamma(a)} > (1 - e^{-d_a x})^a, \quad 0 \leq x < \infty, a > 1, \quad (36)$$

where  $d_a = [\Gamma(1 + a)]^{-1/a}$ . Thus, we have

$$\left[ \frac{1}{\Gamma(M)} \Phi\left(M, \frac{\hat{\gamma}}{t}\right) \right]^B > \left[ 1 - e^{-d_a \frac{\hat{\gamma}}{t}} \right]^{BM}. \quad (37)$$

Then, Eq. (34) can be rewritten as

$$\begin{aligned} P_{\text{DEPS}}^{\text{U}}(\tilde{\gamma}) &> \int_0^\infty e^{-t} \left[ \frac{\Phi\left(M, \frac{\hat{\gamma}}{t}\right)}{\Gamma(M)} \right]^B dt \\ &> \sum_{b=0}^{BM} (-1)^b \int_0^\infty e^{-t - \frac{bd_M \hat{\gamma}}{t}} dt. \end{aligned} \quad (38)$$

$$P_{\text{DEPS}}^{\text{U}}(\tilde{\gamma}) = \int_{x=0}^{\infty} (1 - \mu^2) \exp[-(1 - \mu^2)x] \prod_{b=1}^B \int_{r_b=0}^{\infty} \frac{(r_b)^{U-1} \exp(-r_b)}{\Gamma(U)} \left[ 1 - Q_U \left( \sqrt{\frac{2\mu^2 r_b}{1 - \mu^2}}, \sqrt{\frac{\tilde{\gamma}}{2x}} \right) \right]^{L_b} dr_b dx \quad (31)$$

$$P_{\text{UCPS}}^{\text{U}}(\tilde{\gamma}) = \frac{(1 - \mu^2)^M}{\Gamma(M)} \int_{y=0}^{\infty} \exp(-y + \mu^2 y) y^{M-1} dy \prod_{b=1}^B \int_{r_b=0}^{\infty} e^{-r_b} \left[ 1 - Q_1 \left( \sqrt{\frac{2\mu^2 r_b}{1 - \mu^2}}, \sqrt{\frac{\tilde{\gamma}}{2y}} \right) \right]^{L_b} dr_b \quad (44)$$

Next, Eq. (35) can be derived by applying the result of [31, Eq. (3.471.9)], which completes the proof. ■

*Corollary 5:* The uplink WDT outage probability  $P_{\text{DEPS}}^{\text{U}}$  with the uplink SNR threshold  $\gamma_{\text{th}}^{\text{U}}$ , and decreases with the user number  $M$  and transmission power  $P_t$ .

#### D. Outage Probabilities under the UCPS Strategy

In this section, we will analyze the outage performance under the UCPS strategy. By applying the UCPS strategy, the receiver switches the port based solely on the uplink channel  $h_n^{(m)}$ , selecting the port that has the best uplink channel gain. When the user  $m$  applies the UCPS strategy, it selects the optimal antenna port  $n^*$  having the maximum  $|h_n^{(m)}|^2$  as

$$n^* = \arg \max_n |h_n^{(m)}|^2. \quad (39)$$

Thus, the downlink WDT outage probability is expressed as

$$\begin{aligned} P_{\text{UCPS}}^{\text{D}}(\gamma_{\text{th}}^{\text{D}}) &= \Pr \left( \gamma_{\text{D},n^*}^{(m)} < \gamma_{\text{th}}^{\text{D}} \mid n^* = \arg \max_n |h_n^{(m)}|^2 \right) \\ &= \Pr \left( \frac{X_{n^*}}{Y_{n^*}} < \gamma_{\text{th}}^{\text{D}} \mid n^* = \arg \max_n \beta_n \right). \end{aligned} \quad (40)$$

*Theorem 5:* The downlink WDT outage probability under the UCPS strategy is derived as

$$P_{\text{UCPS}}^{\text{D}}(\gamma_{\text{th}}^{\text{D}}) = 1 - \frac{1}{(\gamma_{\text{th}}^{\text{D}} + 1)^{M-1}}. \quad (41)$$

*Proof:* Due to the independence between the uplink and downlink channels, selecting the port based on the uplink channel is equivalent to the outage probability in single antenna scenario. Thus, Eq. (40) is then simplified as

$$P_{\text{UCPS}}^{\text{D}}(\gamma_{\text{th}}^{\text{D}}) = \Pr \left( \frac{X_{n^*}}{Y_{n^*}} < \gamma_{\text{th}}^{\text{D}} \right), \forall n^*. \quad (42)$$

Similar to the case of DEPS strategy, Eq. (42) is further derived. ■

In what follows, we will analyze the uplink WDT outage probability, which is expressed as

$$\begin{aligned} P_{\text{UCPS}}^{\text{U}}(\gamma_{\text{th}}^{\text{U}}) &= \Pr \left( \gamma_{\text{U},n^*}^{(m)} < \gamma_{\text{th}}^{\text{U}} \mid n^* = \arg \max_n |h_n^{(m)}|^2 \right) \\ &= \Pr \left( \alpha_{n^*} \beta_{n^*} < \tilde{\gamma} \mid n^* = \arg \max_n \beta_n \right) \\ &= \Pr \left( \max_n \beta_n < \frac{\tilde{\gamma}}{\alpha_{n^*}} \right). \end{aligned} \quad (43)$$

*Theorem 6:* The uplink WDT outage probability under the UCPS strategy is expressed as in Eq. (44).

*Proof:* Please refer to Appendix G for the detailed proof. ■

*Corollary 6:* The uplink WDT outage probability under the UCPS strategy can be approximated as

$$\begin{aligned} P_{\text{UCPS}}^{\text{U}}(\tilde{\gamma}) &\approx \frac{(1 - \mu^2)^M}{2^{M-1} \Gamma(M)} \sum_{b=0}^B \binom{B}{b} (-1)^b \left( \frac{b\tilde{\gamma}}{\mu^2} \right)^{\frac{M}{2}} \\ &\quad \times K_M \left( \frac{1 - \mu^2}{\mu} \sqrt{b\tilde{\gamma}} \right). \end{aligned} \quad (45)$$

*Proof:* By using the SFA, Eq. (44) is re-formulated as

$$\begin{aligned} P_{\text{UCPS}}^{\text{U}}(\tilde{\gamma}) &\approx \frac{(1 - \mu^2)^M}{\Gamma(M)} \int_{y=0}^{\infty} e^{-(1-\mu^2)y} y^{M-1} dy \prod_{b=1}^B \int_{r_b=0}^{\infty} \frac{\tilde{\gamma}^{1-\mu^2}}{4\mu^2 y} e^{-r_b} dr_b \\ &= \frac{(1 - \mu^2)^M}{\Gamma(M)} \int_{y=0}^{\infty} e^{-(1-\mu^2)y} y^{M-1} \left[ 1 - e^{-\frac{\tilde{\gamma}(1-\mu^2)}{4\mu^2 y}} \right]^B dy. \end{aligned} \quad (46)$$

Then, Eq. (45) is derived by applying the binomial theorem and the result of Eq. (3.471.9) in [33], which completes the proof. ■

*Proposition 3:* Similar to Proposition 1, the uplink WDT outage probability under UCPS strategy is lower bounded by

$$P_{\text{UCPS}}^{\text{U}}(\tilde{\gamma}) > \frac{1}{2^{M-1} \Gamma(M)} \sum_{b=0}^N (-1)^b \left( \sqrt{b\tilde{\gamma}} \right)^M K_M \left( \sqrt{b\tilde{\gamma}} \right). \quad (47)$$

*Corollary 7:* As  $\gamma_{\text{th}}^{\text{U}}$  increases, the uplink WDT outage probability  $P_{\text{UCPS}}^{\text{U}}$  increases. As  $P_t$  or  $B$  increases, the uplink WDT outage probability  $P_{\text{UCPS}}^{\text{U}}$  decreases.

#### E. Outage Probabilities under the USPS Strategy

In this section, we study a port selection strategy based on the received SNR at the HAP from the user  $m$ , referred to as the USPS strategy. This strategy requires knowledge of both the downlink signals received by user  $m$  and the transmitted uplink signal. If the USPS strategy is applied, the user selects the optimal antenna port  $n^*$  that achieves the maximum of the received SNR at the HAP, which is expressed as

$$n^* = \arg \max_n \gamma_{\text{U},n}^{(m)} = \arg \max_n |h_n^{(m)}|^2 \sum_{\tilde{m}=1}^M |g_n^{(\tilde{m},m)}|^2. \quad (48)$$

$$P_{\text{USPS}}^{\text{U}}(\tilde{\gamma}) = \prod_{b=1}^B \int_0^\infty \int_0^\infty \frac{r_b^{M-1} e^{-\tilde{r}_b - r_b}}{\Gamma(M)} \left[ 1 - \int_{z=0}^\infty Q_M \left( \sqrt{\frac{2\mu^2 r_b}{1-\mu^2}}, \sqrt{\frac{\tilde{\gamma}}{2z}} \right) e^{-z - \frac{\mu^2 \tilde{r}_b}{1-\mu^2}} I_0 \left( 2\sqrt{\frac{\mu^2 \tilde{r}_b z}{1-\mu^2}} \right) dz \right]^{L_b} dr_b d\tilde{r}_b \quad (53)$$

$$\begin{aligned} P_{\text{USPS}}^{\text{U}}(\gamma_{\text{th}}^{\text{U}}) &= P \left( \arg \max_n \alpha_n \beta_n < \tilde{\gamma} \right) = \int_0^\infty \dots \int_0^\infty F_{\alpha_n | \beta_n} \left( \frac{\tilde{\gamma}}{y_1}, \dots, \frac{\tilde{\gamma}}{y_N} \right) f_{\beta_n}(y_1, \dots, y_N) dy_1, \dots, dy_N \\ &\stackrel{(a)}{=} \prod_{b=1}^B \int_0^\infty \frac{r_b^{M-1} e^{-\frac{\tilde{r}_b + r_b}{2}}}{2^{M+1} \Gamma(M)} \left[ 1 - \int_{y=0}^\infty Q_M \left( \sqrt{\frac{\mu^2 r_b}{1-\mu^2}}, \sqrt{\frac{\tilde{\gamma}}{y}} \right) \frac{1}{2} \exp \left[ -\frac{y + \frac{\mu^2 \tilde{r}_b}{1-\mu^2}}{2} \right] I_0 \left( \sqrt{\frac{\mu^2 \tilde{r}_b y}{1-\mu^2}} \right) dy \right]^{L_b} dr_b d\tilde{r}_b \end{aligned} \quad (54)$$

Firstly, the downlink WDT outage probability based on the USPS strategy is expressed as

$$\begin{aligned} P_{\text{USPS}}^{\text{D}}(\gamma_{\text{th}}^{\text{D}}) &= \Pr \left( \gamma_{\text{D}, n^*}^{(m)} < \gamma_{\text{th}}^{\text{D}} \mid n^* = \arg \max_n \gamma_{\text{U}, n}^{(m)} \right) \\ &= \Pr \left( \frac{X_{n^*}}{Y_{n^*}} < \gamma_{\text{th}}^{\text{D}} \mid n^* = \arg \max_n \beta_n \alpha_n \right), \end{aligned} \quad (49)$$

Next, we investigate the downlink WDT outage probability in the following theorem.

*Theorem 7:* The downlink WDT outage probability by applying the USPS strategy is approximated as

$$P_{\text{USPS}}^{\text{D}}(\gamma_{\text{th}}^{\text{D}}) \approx 1 - \frac{1}{(\gamma_{\text{th}}^{\text{D}} + 1)^{M-1}}. \quad (50)$$

*Proof:* Since  $\mu^2$  is close to 1, using the result of Lemma 2,  $X_{n^*}/Y_{n^*}$ ,  $\alpha_n$  and  $\beta_n$  becomes independent to each other. Then, the downlink WDT outage probability under the USPS strategy can be approximated by that of a single traditional antenna as

$$P_{\text{USPS}}^{\text{D}}(\gamma_{\text{th}}^{\text{D}}) \approx \Pr \left( \gamma_{\text{D}, n^*}^{(m)} = \frac{X_{n^*}}{Y_{n^*}} < \gamma_{\text{th}}^{\text{D}} \right), \forall n^*. \quad (51)$$

After that, Eq. (50) can be obtained by following the same steps as the proof of Theorem 3. ■

Then, we aim to study the uplink WDT outage probability under the USPS strategy, which is expressed as

$$\begin{aligned} P_{\text{USPS}}^{\text{U}}(\gamma_{\text{th}}^{\text{U}}) &= \Pr \left( \arg \max_n \gamma_{\text{U}, n}^{(m)} < \gamma_{\text{th}}^{\text{U}} \right) \\ &= \Pr \left( \arg \max_n \alpha_n \beta_n < \tilde{\gamma} \right). \end{aligned} \quad (52)$$

After that, we investigate the uplink WDT outage probability in the following theorem.

*Theorem 8:* The uplink WDT outage probability under the USPS strategy is formulated as in Eq. (53).

*Proof:* The uplink WDT outage probability under the USPS strategy is formulated as in Eq. (54), where (a) uses the results of Eq. (E.3) and Eq. (G.2) as well as the variable substitutions. Then, Eq. (53) is obtained, which completes the proof. ■

Then, by applying the Lemma 1, the closed-form of the uplink WDT outage probability under the USPS strategy is given in the following Corollary.

*Corollary 8:* The uplink WDT outage probability under the USPS strategy can be further approximated as

$$P_{\text{USPS}}^{\text{U}}(\tilde{\gamma}) \approx \left[ 1 - \frac{\left( \frac{1-\mu^2}{\mu^2} \sqrt{\tilde{\gamma}} \right)^M}{2^{M-1} \Gamma(M)} K_M \left( \frac{1-\mu^2}{\mu^2} \sqrt{\tilde{\gamma}} \right) \right]^B. \quad (55)$$

*Proof:* With the aid of the SFA, Eq. (53) is re-formulated as

$$\begin{aligned} P_{\text{USPS}}^{\text{U}}(\tilde{\gamma}) &\approx \prod_{b=1}^B \int_0^\infty \int_0^\infty \frac{r_b^{M-1} e^{-\tilde{r}_b - r_b}}{\Gamma(M)} \left[ 1 - \int_{\frac{\tilde{\gamma}(1-\mu^2)}{4\mu^2 r_b}}^\infty e^{-y - \frac{\mu^2 \tilde{r}_b}{1-\mu^2}} I_0 \left( 2\sqrt{\frac{\mu^2 \tilde{r}_b y}{1-\mu^2}} \right) dy \right]^{L_b} dr_b d\tilde{r}_b. \end{aligned} \quad (56)$$

Note that the generalized Marcum Q-function can be alternatively defined as a finite integral. Thus, Eq. (56) can be rewritten as

$$\begin{aligned} P_{\text{USPS}}^{\text{U}}(\tilde{\gamma}) &= \prod_{b=1}^B \int_0^\infty \int_0^\infty \frac{r_b^{M-1} e^{-\tilde{r}_b - r_b}}{\Gamma(M)} \times \\ &\left[ 1 - Q_1 \left( \sqrt{\frac{2\mu^2 \tilde{r}_b}{1-\mu^2}}, \sqrt{\frac{\tilde{\gamma}(1-\mu^2)}{2\mu^2 r_b}} \right) \right]^{L_b} dr_b d\tilde{r}_b. \end{aligned} \quad (57)$$

Then, due to the presence of the Marcum-Q function, we can apply the SFA once again to approximate Eq. (57) as

$$P_{\text{USPS}}^{\text{U}}(\tilde{\gamma}) \approx \prod_{b=1}^B \int_{r_b=0}^\infty \frac{r_b^{M-1} e^{-r_b}}{\Gamma(M)} \int_{\tilde{r}_b=0}^{\frac{\tilde{\gamma}(1-\mu^2)^2}{4\mu^4 r_b}} e^{-\tilde{r}_b} d\tilde{r}_b dr_b. \quad (58)$$

Finally, Eq. (55) is obtained by applying the result of Eq. (3.471.9) in [31], which completes the proof. ■

*Proposition 4:* The uplink WDT outage probability under USPS strategy is lower bounded as

$$P_{\text{USPS}}^{\text{U}}(\tilde{\gamma}) > \left[ 1 - \frac{\left( \sqrt{\tilde{\gamma}} \right)^M}{2^{M-1} \Gamma(M)} K_M \left( \sqrt{\tilde{\gamma}} \right) \right]^B. \quad (59)$$

*Proof:* Please refer to Appendix H for the detailed proof. ■

*Remark 2:* As shown in Eq. (55), the outage probability decreases exponentially with an increase in  $B$ . It has been



TABLE I  
OUTAGE PERFORMANCE METRICS SUMMARY

|              | DSPS strategy                        | DEPS strategy   | UCPS strategy   | USPS strategy   |
|--------------|--------------------------------------|---|---|---|
| Downlink WDT | Theorem 1 (GLQ)<br>Corollary 2 (SFA) | Theorem 3 (Approx.)   | Theorem 5 (Ana.)  | Theorem 7 (Approx.)   |
| Uplink WDT   | Theorem 2 (Approx.)                  | Theorem 4 (GLQ)<br>Corollary 4 (SFA)<br>Proposition 1 (Lower bound) | Theorem 6 (GLQ)<br>Corollary 6 (SFA)<br>Proposition 3 (Lower bound) | Theorem 8 (GLQ)<br>Corollary 8 (SFA)<br>Proposition 4 (Lower bound) |

demonstrated that  $B$  can be approximated by  $2W$  for large  $N$  [30]. Therefore, with a fixed antenna size  $W$  and increasing port number  $N$ , the outage probability initially decreases and then converges due to the limitation imposed by  $W$ . Similarly, with a fixed  $N$  and increasing  $W$ , the uplink WDT outage probability decreases as the distance between ports increases, eventually converging to the derived lower bound when the wireless channels among ports become independent.

*Corollary 9:* As  $\gamma_{th}^U$  increases, the uplink WDT outage probability  $P_{USPS}^U$  increases. As  $M$  or  $P_t$  increases, the uplink WDT outage probability  $P_{USPS}^U$  decreases.

#### IV. NUMERICAL RESULTS

This section presents results obtained through Gauss-Laguerre quadrature (GLQ) [34] for the theoretical expressions in Theorems 1, 4, 6, and 8, along with results derived using the SFA in Corollaries 2, 4, 6, and 8. We also discuss the approximations in Theorems 2, 3, and 7, and include lower bounds from Propositions 1, 3, and 4 for a comprehensive analysis. Monte Carlo simulations are used to validate the theoretical results, evaluating the outage performance of FAMA-assisted WPCN. A summary of simulation-based performance metrics is provided in Table I. The simulation parameters are as follows: AWGN variance is  $\sigma_w^2 = -50$  dBm, IDET and WDT phases both last 0.5s, with identical path loss between HAP antenna and users. Other parameter settings are detailed in each figure.

##### A. Downlink WDT outage probability

As shown in the Figs. 3 and 4, the outage probability increases with the rise of  $M$  or  $\gamma_{th}^D$ , expectably. It can be observed that the downlink WDT outage performance under the DSPS strategy outperforms that of the USPS, DEPS, and UCPS strategies. This is because the DSPS strategy selects the port with the least interference. Besides, the theoretical analysis for DSPS by using GLQ matches well with the simulation results. The approximate closed-forms of the outage probabilities under the USPS and DEPS strategies closely match the actual outage probabilities, demonstrating the effectiveness of the approximation. The downlink WDT outage probability in Theorem 5 is shown to be in complete agreement with the simulated values, thereby verifying the correctness of our theoretical derivation. Moreover, under the DSPS strategy, we employ the SFA approximation twice to derive a closed-form expression. While the results are not fully consistent with simulation results and GLQ calculations, the approximation effectively captures the downlink WDT outage performance trends of the proposed system without the need for computing multiple integrals.

##### B. Uplink WDT outage probability

Fig. 5 illustrates the uplink WDT outage probability versus transmit power  $P_t$  under the four port selection strategies. The results obtained using GLQ closely match the simulation outcomes, validating the correctness of the theoretical analysis. Although the SFA-derived analytical solution shows some discrepancy with the simulation results under the USPS and UCPS strategies, the closed-form expressions effectively capture the system's performance without requiring multiple integrals. As expected, the uplink WDT outage probability decreases as  $P_t$  increases for all four strategies. It can also be observed that among the four proposed port selection strategies, the DSPS strategy exhibits the poorest uplink WDT performance, while the USPS strategy achieves the best performance. Interestingly, although the DEPS strategy selects the port that harvests the most EHP, the uplink WDT outage probability is worse than the UCPS strategy, which selects the port based solely on the uplink channel. The results suggest that the UCPS strategy could be an acceptable candidate for the system to achieve a good performance, while it does not require knowledge of the double-side channel information and thus is relatively simpler to implement.

Fig. 6 shows the effect of the uplink SNR threshold on the uplink WDT outage probability. The performance under these four strategies is consistent with those shown in Fig. 5, *i.e.*, USPS strategy performs the best compared to the other three strategies. Apparently, as  $\gamma_{th}^U$  increases, the uplink WDT outage probability also increases, which agrees with the Theorem 2, Corollaries 4, 6, and 8. It is worth noting that for the UCPS strategy, the outage probability calculated using the GLQ shows significant errors when  $\gamma_{th}^U$  is large. This is because, as  $\gamma_{th}^U$  increases, the value of the inner integral function in Eq. (44) gradually grows, leading to tail-end errors that affect the accuracy. In contrast, the SFA-based approach effectively captures the performance trends across all strategies.

Fig. 7 is provided to further discuss the effect of  $M$  on the uplink WDT performance. It can be observed that as the number of users  $M$  increases, the uplink outage probability decreases. This is because more users result in more energy being collected, leading to a better performance, which agrees with the Theorem 2, Corollaries 4, 6, and 8. Besides, under the DSPS and DEPS strategies, the improvement in performance with an increasing number of users is much smaller compared to the other two strategies. This is because the UCPS and USPS strategies directly impact the uplink WDT performance, whereas the DSPS and DEPS strategies influence the uplink WDT performance indirectly by affecting the amount of energy harvested during the downlink IDET phase.

Fig. 8 explores the impact of antenna size  $W$  on the uplink WDT performance. Under the DSPS strategy, the uplink WDT outage probability remains unchanged as  $W$  varies, consistent with (25), which is independent of  $W$ . Under the DEPS strategy, the decrease in outage probability is minimal as  $W$  increases, as the system cannot fully exploit the diversity introduced by the FA. In contrast, the outage performance under the UCPS and USPS strategies improves more noticeably as  $W$  increases. This is because, when the number of ports  $N$

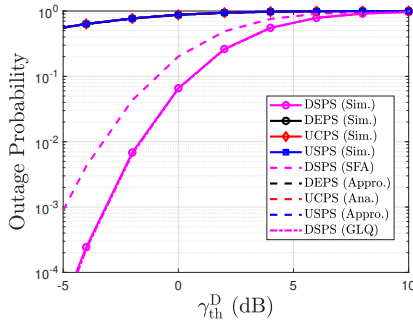


Fig. 3. Downlink WDT outage probability versus  $\gamma_{th}^D$ ;  $M = 4$ ,  $N = 100$ ,  $W = 5$ ,  $\mu^2 = 0.97$ .

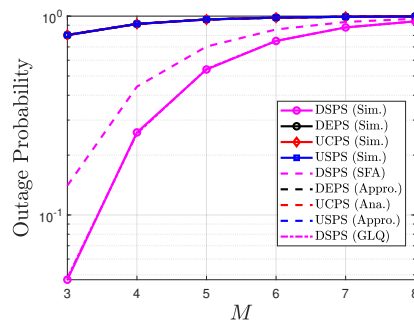


Fig. 4. Downlink WDT outage probability versus  $M$ ;  $\gamma_{th}^D = 1$  dB,  $N = 50$ ,  $W = 4$ ,  $\mu^2 = 0.97$ .

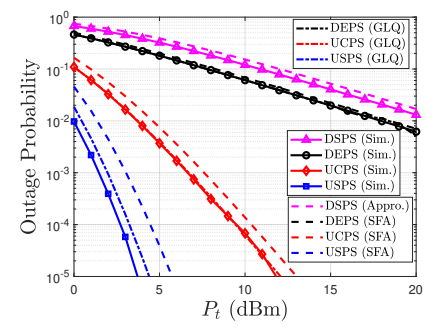


Fig. 5. Uplink WDT outage probability versus transmit power  $P_t$ ;  $N = 50$ ,  $M = 4$ ,  $W = 4$ ,  $\mu^2 = 0.97$ ,  $\gamma_{U,th}^{(m)} = 10$  dB.

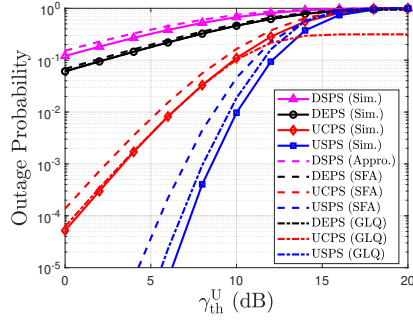


Fig. 6. Uplink WDT outage probability versus uplink SNR threshold  $\gamma_{th}^U$ ;  $P_t = 0$  dBm,  $N = 50$ ,  $M = 4$ ,  $W = 4$ ,  $\mu^2 = 0.97$ .

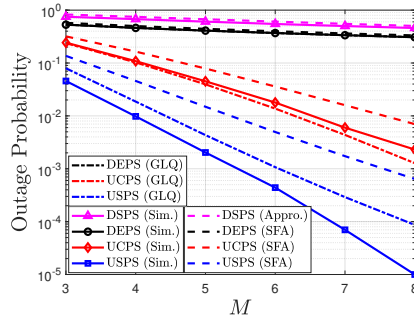


Fig. 7. Uplink WDT outage probability versus  $M$ ;  $P_t = -10$  dBm,  $\gamma_{th}^U = 2$  dB,  $N = 100$ ,  $W = 5$ ,  $\mu^2 = 0.97$ .

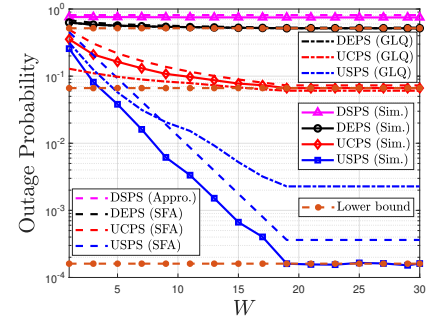


Fig. 8. Uplink WDT outage probability versus  $W$ ;  $M = 5$ ,  $N = 50$ ,  $P_t = -5$  dBm,  $\mu^2 = 0.97$ , and  $\gamma_{th}^U = 2$  dB.

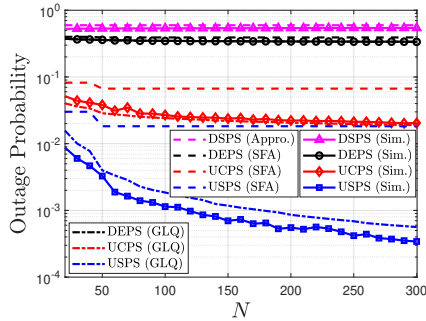


Fig. 9. Uplink WDT outage probability versus  $N$ ;  $M = 5$ ,  $P_t = -5$  dBm,  $W = 3$ ,  $\gamma_{th}^U = 2.5$  dB, and  $\mu^2 = 0.97$ .

is fixed, increasing  $W$  reduces the correlation between ports (increasing  $B$ ), resulting in better performance. However, as  $W$  grows continuously, the outage probabilities under DEPS, UCPS, and USPS strategies gradually approach the derived lower bound. This occurs because, when  $N$  is fixed, a larger  $W$  increases the distance between ports, eliminating the correlation, making the  $N$ -port FA equivalent to  $N$  independent single-antenna systems, as shown in Proposition 1, Proposition 3, and Proposition 4.

Fig. 9 investigates the impact of another key parameter, port number  $N$ , on the uplink WDT outage performance. Similar to Fig. 8, under the DSPS strategy, the uplink WDT outage probability remains constant as  $N$  increases, which is consistent with Eq. (25). Moreover, under the DEPS, UCPS,

and USPS strategies, the outage probability decreases initially and then gradually saturates as  $N$  increases from 20 to 300. This is because when we increase  $N$  initially, additional diversity is introduced ( $B$  gets bigger). However, if  $N$  continues to increase, the WDT performance exhibits a flat trend. In this case, the ports become closer together, which results in a stronger correlation, and the WDT performance is mainly constrained by the FA size,  $W$ .

## V. CONCLUSION

This paper analyzed the outage performance of a FAMA-assisted WPCN system under four port selection strategies: DSPS, DEPS, UCPS, and USPS, each associated with different implementation complexities and CSI requirements. The closed-form expressions for downlink WDT outage probabilities were derived. Besides, the exact expressions of the uplink WDT outage probabilities were derived, while the corresponding approximate expressions were also presented by using the SFA. Monte Carlo simulation results validated the accuracy and effectiveness of our theoretical results. It can be concluded that the system achieves a better downlink WDT performance under the DSPS strategy, while the other three strategies yield nearly identical and relatively poor performance. Further, the system achieves a better uplink WDT performance under the USPS strategy, whereas the performance is worst when using the DSPS strategy. Moreover, the UCPS strategy is a better candidate to achieve a trade-off between the uplink WDT performance and the implementation complexity.

$$\begin{aligned}
 P_{\text{DSPA}}^{\text{D}}(\gamma_{\text{th}}^{\text{D}}) &\stackrel{(a)}{=} \prod_{b=1}^B \int_0^\infty \int_0^\infty \frac{r_b^{M-2} e^{-\frac{\tilde{r}_b+r_b}{2}}}{2^M \Gamma(M)} \left[ 1 - \frac{1}{2} \int_{y=0}^\infty Q_1 \left( \sqrt{\frac{\mu^2 r_b}{1-\mu^2}}, \sqrt{\gamma_{\text{th}}^{\text{D}} y} \right) \left( \frac{y(1-\mu^2)}{\mu^2 \tilde{r}_b} \right)^{\frac{M-2}{2}} \right. \\
 &\quad \left. \times \exp \left( -\frac{y_n + \frac{\mu^2}{1-\mu^2} \tilde{r}_b}{2} \right) I_{M-2} \left( \sqrt{\frac{\mu^2 \tilde{r}_b y}{1-\mu^2}} \right) dy \right]^{L_b} dr_b d\tilde{r}_b \\
 &\stackrel{(b)}{\approx} \prod_{b=1}^B \int_0^\infty \int_0^\infty \frac{r_b^{M-2} e^{-\frac{\tilde{r}_b+r_b}{2}}}{2^M \Gamma(M)} \left[ 1 - \frac{1}{\left( \frac{\mu^2 \tilde{r}_b}{1-\mu^2} \right)^{\frac{M-2}{2}}} \int_{x=0}^{\sqrt{\frac{\mu^2 r_b}{(1-\mu^2) \gamma_{\text{th}}^{\text{D}}}}} x^{M-1} e^{-x^2 - \frac{\mu^2}{1-\mu^2} \tilde{r}_b} I_{M-2} \left( \sqrt{\frac{\mu^2 \tilde{r}_b}{1-\mu^2} x} \right) dx \right]^{L_b} dr_b d\tilde{r}_b \\
 &\stackrel{(c)}{=} \prod_{b=1}^B \int_0^\infty \frac{r_b^{M-2} e^{-\tilde{r}_b - r_b}}{\Gamma(M)} \left[ Q_{M-1} \left( \sqrt{\frac{2\mu^2 r_b}{1-\mu^2}}, \sqrt{\frac{2\mu^2 r_b}{(1-\mu^2) \gamma_{\text{th}}^{\text{D}}}} \right) \right]^{L_b} dr_b d\tilde{r}_b
 \end{aligned} \tag{A.1}$$

APPENDIX A  
PROOF OF COROLLARY 1

We can re-formulate the downlink WDT outage probability as in Eq. (A.1), where (a) uses the result of Eq. (54) in [30], (b) applies the SFA and the variable substitution, and (c) accounts for the fact that the generalized Marcum Q-function can alternatively be defined as a finite integral. Thus, the proof of corollary 1 ends.

APPENDIX B  
PROOF OF LEMMA 2

When  $\mu^2 = 1$ , we have

$$X_n = \left( x_{b(n)}^{(m,m,\text{D})} \right)^2 + \left( y_{b(n)}^{(m,m,\text{D})} \right)^2. \tag{B.1}$$

$$Y_n = \sum_{\substack{\tilde{m} \neq m \\ \tilde{m}=1}}^M \left( x_{b(n)}^{(\tilde{m},m,\text{D})} \right)^2 + \left( y_{b(n)}^{(\tilde{m},m,\text{D})} \right)^2. \tag{B.2}$$

Then, the  $X_n$  is exponentially distributed with probability density function (PDF)

$$f_{X_n}(x) = e^{-x/2}, \tag{B.3}$$

and  $Y_n$  follows a central chi-squared distribution with  $2(M-1)$  degrees of freedom. Thus, we have

$$f_{Y_n}(y) = \frac{1}{2^{M-1} \Gamma(M-1)} y^{M-2} e^{-y/2}. \tag{B.4}$$

After that, we use the transformations:  $V_1 = X_n + Y_n$  and  $V_2 = X_n/Y_n$ . Since  $X_n$  and  $Y_n$  are independent,  $V_1$  is a central Chi-square distribution with the PDF

$$f_{V_1}(v_1) = \frac{1}{2^M \Gamma(M)} v_1^{M-1} e^{-v_1/2}, \tag{B.5}$$

and  $V_2$  is a Beta prime distribution with the PDF

$$f_{V_2}(v_2) = \frac{M-1}{(1+v_2)^M}. \tag{B.6}$$

Then, we have  $X_n = \frac{V_1 V_2}{1+V_2}$  and  $Y_n = \frac{V_1}{1+V_2}$ . By formulating the absolute value of the Jacobian determinant as  $|J| = \frac{V_1}{(1+V_2)^2}$ , the joint PDF of  $V_1$  and  $V_2$  is

$$f_{V_1, V_2}(v_1, v_2) = f_{X_n, Y_n}(x, y) \cdot |J|. \tag{B.7}$$

Finally, we have the following results by substituting the PDF of  $X_n, Y_n$  as

$$f_{V_1, V_2}(v_1, v_2) = \underbrace{\frac{v_1^{M-1} e^{-v_1/2}}{2^M \Gamma(M)}}_{\text{PDF of } V_1} \cdot \underbrace{\frac{M-1}{(1+v_2)^M}}_{\text{PDF of } V_2}. \tag{B.8}$$

Since the joint PDF factorizes into the product of marginal PDFs,  $V_1$  and  $V_2$  are independent. Therefore, the proof of Lemma 2 ends.

APPENDIX C  
PROOF OF THEOREM 2

To evaluate the uplink WDT outage probability, we first exploit an important integral involving the Marcum-Q function and exp established in [33, Eq. (18)] as

$$\begin{aligned}
 \mathcal{F}(a, b, c) &= \int_0^\infty Q_1(a\sqrt{x}, b) e^{-cx} dx \\
 &= \frac{e^{-\frac{b^2}{2}}}{c} + \frac{e^{-\frac{cb^2}{a^2+2c}}}{c} \left[ 1 - e^{-\frac{a^2 b^2}{2a^2+4c}} \right].
 \end{aligned} \tag{C.1}$$

where  $a, b$  and  $c$  are all the constants. Since  $\mu^2$  is close to 1, we can approximate  $X_n$  and  $Y_n$  as

$$X_n \approx \left( x_{b(n)}^{(m,m,\text{D})} \right)^2 + \left( y_{b(n)}^{(m,m,\text{D})} \right)^2. \tag{C.2}$$

$$Y_n \approx \sum_{\substack{\tilde{m} \neq m \\ \tilde{m}=1}}^M \left( x_{b(n)}^{(\tilde{m},m,\text{D})} \right)^2 + \left( y_{b(n)}^{(\tilde{m},m,\text{D})} \right)^2. \tag{C.3}$$

Then, with the aid of lemma 2,  $X_n + Y_n$  and  $\frac{X_n}{Y_n}$  can be approximated as independent. Furthermore, due to the independence of the uplink and downlink channels,  $X_n + Y_n$ ,

$$\begin{aligned}
 P_{\text{DSPS}}^{\text{U}}(\gamma_{\text{th}}^{\text{U}}) &\stackrel{(a)}{\approx} P\left(\beta_{n^*} < \frac{\tilde{\gamma}}{\alpha_{n^*}}\right) \\
 &\stackrel{(b)}{=} \int_{r=0}^{\infty} \frac{1}{2} e^{-r/2} \int_0^{\infty} \left[1 - Q_1\left(\sqrt{\frac{\mu^2 r}{1-\mu^2}}, \sqrt{y}\right)\right] \times \frac{1}{2^M \Gamma(M)} y^{U-1} \exp\left(-\frac{y}{2}\right) dy dr \\
 &\stackrel{(c)}{=} 1 - \frac{1}{2^{M+1} \Gamma(M)} \int_{r=0}^{\infty} \int_{y=0}^{\infty} \exp\left(-\frac{r}{2}\right) Q_1\left(\sqrt{\frac{\mu^2 r}{1-\mu^2}}, \sqrt{\frac{\tilde{\gamma}}{y}}\right) y^{U-1} \exp\left(-\frac{y}{2}\right) dy dr \\
 &\stackrel{(d)}{=} 1 - \frac{1}{\Gamma(M)} \int_{y=0}^{\infty} y^{M-1} \exp\left(-y - \frac{\tilde{\gamma}(1-\mu^2)}{4y}\right) dy
 \end{aligned} \tag{C.7}$$

$\frac{X_n}{Y_n}$  and  $\beta_n$  are mutually independent. As a result, Eq. (23) can be simplified as

$$P_{\text{DSPS}}^{\text{U}}(\gamma_{\text{th}}^{\text{U}}) \approx P(\beta_{n^*} \alpha_{n^*} < \tilde{\gamma}), \forall n^*. \tag{C.4}$$

After approximation,  $\alpha_n$  follows central Chi-square distribution with PDF as in Eq. (B.5). By defining  $\tilde{r} = (x^{(m,U)})^2 + (y^{(m,U)})^2$ , which follows an exponential distribution, the unconditioned PDF of  $\beta_{n^*}$  is then expressed as

$$f_{\beta_{n^*}}(t) = \int_0^{\infty} \frac{1}{2} e^{-\frac{\tilde{r}}{2}} e^{-\frac{t+\frac{\mu^2}{1-\mu^2}\tilde{r}}{2}} I_0\left(\sqrt{\frac{\mu^2 \tilde{r} t}{1-\mu^2}}\right) d\tilde{r}. \tag{C.5}$$

And the unconditioned cumulative distribution function (CDF) of  $\beta_{n^*}$  is then formulated as

$$F_{\beta_{n^*}}(t) = \int_0^{\infty} \frac{1}{2} e^{-\frac{\tilde{r}_b}{2}} \left[1 - Q_1\left(\sqrt{\frac{\mu^2 \tilde{r}_b}{1-\mu^2}}, \sqrt{t}\right)\right] d\tilde{r}_b. \tag{C.6}$$

Then, the uplink WDT outage probability can be formulated as in Eq. (C.7), where (a) uses the fact that  $\beta_{n^*}$  and  $\alpha_{n^*}$  are independent, (b) uses the results of Eq. (B.5) and Eq. (C.6), (c) uses the fact that the total probability of a central Chi-square random variable is 1, (d) is obtained by setting  $a = \sqrt{\frac{\mu^2}{1-\mu^2}}$ ,  $b = \sqrt{\frac{\tilde{\gamma}}{y}}$  and  $c = \frac{1}{2}$  in Eq. (C.1). Consequently, by applying the result of [31, Eq. (3.471.9)], the uplink WDT outage probability is obtained as in Eq. (25), which completes the proof.

#### APPENDIX D PROOF OF THEOREM 3

When  $\mu^2$  is close to 1, we can approximate  $X_n$  and  $Y_n$  as in Eq. (C.2) and Eq. (C.3), respectively. Then, with the aid of Lemma 2, it can be approximated that  $X_n + Y_n$  and  $\frac{X_n}{Y_n}$  are independent. Then, Eq. (28) can be simplified as

$$P_{\text{DEPS}}^{\text{D}}(\gamma_{\text{th}}^{\text{D}}) \approx \Pr\left(\frac{X_{n^*}}{Y_{n^*}} < \gamma_{\text{th}}^{\text{D}}\right) = \Pr(X_{n^*} < Y_{n^*} \gamma_{\text{th}}^{\text{D}}), \forall n^*. \tag{D.1}$$

Note that  $X_{n^*}$  is exponentially distributed with the CDF

$$F_{X_{n^*}}(x) = 1 - e^{-x/2}. \tag{D.2}$$

and  $Y_{n^*}$  is central Chi-squared distributed with the PDF as in Eq. (B.4). Further, the downlink WDT outage probability by applying the DEPS strategy is then calculated as

$$\begin{aligned}
 P_{\text{DEPS}}^{\text{D}}(\gamma_{\text{th}}^{\text{D}}) &= \int_{y=0}^{\infty} F_{X_{n^*}|Y_{n^*}}(\gamma_{\text{th}}^{\text{D}} y) f_{Y_{n^*}}(y) dy \\
 &= 1 - \frac{1}{2^{M-1} \Gamma(M-1)} \int_{y=0}^{\infty} y^{M-2} e^{-\frac{y+\gamma_{\text{th}}^{\text{D}} y}{2}} dy,
 \end{aligned} \tag{D.3}$$

After applying the result of [31, eq. (3.381.4)], Eq. (29) is then obtained, while the proof is completed.

#### APPENDIX E PROOF OF THEOREM 4

Conditioned on  $r_b = \sum_{\tilde{m}=1}^M (x_b^{(\tilde{m},m,D)})^2 + (y_b^{(\tilde{m},m,D)})^2$  for  $b = 1, \dots, B$ ,  $\alpha_n$  is a non-central Chi-square variable with  $2M$  degrees of freedom. The conditioned PDF of  $\alpha_n$  is then obtained as

$$\begin{aligned}
 f_{\alpha_n|r_b}(x) &= \frac{1}{2} \left(\frac{x(1-\mu^2)}{\mu^2 r_b}\right)^{\frac{M-1}{2}} \exp\left(-\frac{x + \frac{\mu^2}{1-\mu^2} r_b}{2}\right) \\
 &\quad \times I_{M-1}\left(\sqrt{\frac{\mu^2 r_b x}{1-\mu^2}}\right).
 \end{aligned} \tag{E.1}$$

Note that each  $r_b$  for  $b = 1, \dots, B$  is a Chi-square distribution with the PDF of

$$f_{r_b}(r_b) = \frac{r_b^{M-1} e^{-r_b/2}}{2^U \Gamma(M)}, b = 1, \dots, B. \tag{E.2}$$

Then, the unconditioned joint CDF of  $\alpha_n$  is formulated as

$$\begin{aligned}
 F_{\alpha_n}(t_1, \dots, t_N) &= \prod_{b=1}^B \int_0^{\infty} \frac{r_b^{M-1} e^{-r_b/2}}{2^M \Gamma(M)} \prod_{n \in N_b} \frac{1}{2} \left(\frac{t_n(1-\mu^2)}{\mu^2 r_b}\right)^{\frac{M-1}{2}} \\
 &\quad \times \left[1 - Q_M\left(\sqrt{\frac{\mu^2 r_b}{1-\mu^2}}, \sqrt{t_n}\right)\right] dr_b.
 \end{aligned} \tag{E.3}$$

Thus, the uplink WDT outage probability can be reformulated as in Eq. (E.4), where (a) uses the results of Eq. (C.6) and (E.3), (b) accounts for the variable substitution. Besides, due to the fact

$$2 \int_b^{\infty} y \exp(-y^2 - a^2) I_0(2ay) dy = Q_1(\sqrt{2}a, \sqrt{2}b), \tag{E.5}$$

$$\begin{aligned}
 P_{\text{DEPS}}^{\text{U}}(\gamma_{\text{th}}^{\text{U}}) &= P\left(\alpha_1 < \frac{\tilde{\gamma}}{\beta_{n^*}}, \dots, \alpha_N < \frac{\tilde{\gamma}}{\beta_{n^*}}\right) \\
 &= \int_{x=0}^{\infty} F_{\alpha_n|\beta_{n^*}}\left(\frac{\tilde{\gamma}}{x}, \dots, \frac{\tilde{\gamma}}{x}\right) \times f_{\beta_{n^*}}(x) dx \\
 &\stackrel{(a)}{=} \int_{\tilde{r}=0}^{\infty} \frac{1}{2} e^{-\frac{\tilde{r}}{2}} \int_{x=0}^{\infty} \frac{1}{2} e^{-\frac{x+\frac{\mu^2\tilde{r}}{1-\mu^2}}{2}} I_0\left(\sqrt{\frac{\mu^2\tilde{r}x}{1-\mu^2}}\right) d\tilde{r} dx \prod_{b=1}^B \int_{r_b=0}^{\infty} \frac{r_b^{M-1} \exp(-\frac{r_b}{2})}{2^M \Gamma(M)} \left[1 - Q_M\left(\sqrt{\frac{\mu^2 r_b}{1-\mu^2}}, \sqrt{\frac{\tilde{\gamma}}{x}}\right)\right]^{L_b} dr_b \\
 &\stackrel{(b)}{=} \int_{x=0}^{\infty} e^{-x} \int_{\tilde{r}=0}^{\infty} e^{-\frac{1}{1-\mu^2}\tilde{r}} I_0\left(2\sqrt{\frac{\mu^2\tilde{r}x}{1-\mu^2}}\right) d\tilde{r} dx \prod_{b=1}^B \int_{r_b=0}^{\infty} \frac{(r_b)^{M-1} \exp(-r_b)}{\Gamma(M)} \left[1 - Q_M\left(\sqrt{\frac{2\mu^2 r_b}{1-\mu^2}}, \sqrt{\frac{\tilde{\gamma}}{2x}}\right)\right]^{L_b} dr_b
 \end{aligned} \tag{E.4}$$

we have

$$\begin{aligned}
 &\int_{\tilde{r}=0}^{\infty} e^{-\frac{\tilde{r}}{1-\mu^2}} I_0\left(2\sqrt{\frac{\mu^2\tilde{r}x}{1-\mu^2}}\right) d\tilde{r} \\
 &\stackrel{(c)}{=} (1-\mu^2) \int_0^{\infty} r e^{-r^2} I_0\left(2\sqrt{\mu^2 x r}\right) dr \\
 &\stackrel{(d)}{=} (1-\mu^2) \exp(\mu^2 x),
 \end{aligned} \tag{E.6}$$

where (c) accounts for the variable substitution, (d) uses the fact that  $Q_1(\sqrt{2\mu^2 x}, 0) = 1$ . Finally, with the aid of Eq. (E.6), Eq. (E.4) can be further simplified as in Eq. (31), which completes the proof.

#### APPENDIX F PROOF OF PROPOSITION 1

As discussed in [30], a simple bound for FA can be obtained by directly setting  $\mu^2 = 1$ . Then, we have

$$\alpha_n = \sum_{\tilde{m}=1}^M \left(x_{b(n)}^{(\tilde{m}, m, \text{D})}\right)^2 + \left(y_{b(n)}^{(\tilde{m}, m, \text{D})}\right)^2. \tag{F.1}$$

$$\beta_n = \left(x_{b(n)}^{(m, \text{U})}\right)^2 + \left(y_{b(n)}^{(m, \text{U})}\right)^2. \tag{F.2}$$

where all the variables above are independent Gaussian variables having zero mean and variance of 1. Therefore,  $\alpha_n$  is central Chi-square distributed with the joint CDF as

$$F_{\alpha_n}(t_1, \dots, t_B) = \prod_{n=1}^B \frac{\Phi\left(M, \frac{t_n}{2}\right)}{\Gamma(M)}, \tag{F.3}$$

Similarly,  $\beta_n$  is exponentially distributed with the PDF as

$$f_{\beta_n}(y) = \frac{1}{2} e^{-y_n/2}. \tag{F.4}$$

Then, the lower bound is calculated as

$$P_{\text{DEPS}}^{\text{U}}(\hat{\gamma}) = \int_0^{\infty} F_{\alpha_n|\beta_{n^*}}\left(\frac{\hat{\gamma}}{t}, \dots, \frac{\hat{\gamma}}{t}\right) f_{\beta_{n^*}}(t) dt. \tag{F.5}$$

Besides, due to the fact that  $\sum_{b=1}^B L_b = N$ , we have  $B \leq N$ . As a result, Eq. (34) is derived by using the results of Eq. (F.3) and Eq. (F.4), which completes the proof.

#### APPENDIX G PROOF OF THEOREM 6

Conditioned on  $\tilde{r}_b = \sum_{b=1}^B \left(x_b^{(m, \text{U})}\right)^2 + \left(y_b^{(m, \text{U})}\right)^2$ ,  $\beta_n$  is a noncentral Chi-square random variable with 2 degrees of freedom. Note that variables  $\tilde{r}_b, \forall b$  are all independent, and each follows an exponential distribution with the PDF as

$$f_{\tilde{r}_b}(\tilde{r}_b) = \frac{1}{2} e^{-\frac{\tilde{r}_b}{2}}, b = 1, \dots, B. \tag{G.1}$$

Then, the unconditioned joint PDF of  $\beta_n$  is formulated as

$$\begin{aligned}
 f_{\beta_n}(t_1, \dots, t_N) &= \prod_{b=1}^B \int_0^{\infty} \frac{1}{2} e^{-\tilde{r}_b/2} \\
 &\times \prod_{n \in \mathcal{N}_b} \exp\left(-\frac{t_n + \frac{\mu_b^2}{1-\mu_b^2} r_b}{2}\right) I_0\left(\sqrt{\frac{\mu_b^2 r_b t_n}{1-\mu_b^2}}\right) dr_b.
 \end{aligned} \tag{G.2}$$

And the unconditioned joint CDF of  $\beta_n$  is formulated as

$$\begin{aligned}
 F_{\beta_n}(t_1, \dots, t_N) &= \prod_{b=1}^B \int_0^{\infty} \frac{1}{2} e^{-\tilde{r}_b/2} \prod_{n \in \mathcal{N}_b} \left[1 - Q_1\left(\sqrt{\frac{\mu_b^2 r_b}{1-\mu_b^2}}, \sqrt{t_n}\right)\right] dr_b
 \end{aligned} \tag{G.3}$$

Then, the uplink WDT outage probability in Eq. (43) is derived as in Eq. (G.4), where (a) uses the results of Eq. (E.1) and Eq. (G.3), (b) uses the variable substitution. Then, with the aid of some simplifications, Eq. (44) is derived, which completes the proof.

#### APPENDIX H PROOF OF PROPOSITION 4

Similar to Proposition 1, a simple bound can be obtained by directly setting  $\mu^2 = 1$ . Subsequently,  $\alpha_n$  and  $\beta_n$  can be expressed as in Eq. (F.1) and Eq. (F.2), respectively. Therefore, the joint PDF of  $\alpha_n$  is expressed as

$$f_{\alpha_n}(t_1, \dots, t_B) = \prod_{n=1}^B \frac{1}{2^M \Gamma(M)} t_n^{M-1} e^{-t_n/2}, \tag{H.1}$$

and the joint CDF of  $\beta_n$  is expressed as

$$F_{\beta_n}(y_1, \dots, y_B) = \prod_{n=1}^B 1 - e^{-y_n/2}. \tag{H.2}$$

$$\begin{aligned}
 P_{\text{UCPS}}^{\text{U}}(\tilde{\gamma}) &= P\left(\beta_1 < \frac{\tilde{\gamma}}{\alpha_{n^*}}, \dots, \beta_N < \frac{\tilde{\gamma}}{\alpha_{n^*}}\right) \\
 &= \int_0^\infty F_{\beta_n|\alpha_{n^*}}\left(\frac{\tilde{\gamma}}{y}, \dots, \frac{\tilde{\gamma}}{y}\right) f_{\alpha_{n^*}|\tilde{r}}(y) dy \\
 &\stackrel{(a)}{=} \int_{y=0}^\infty \int_{\tilde{r}=0}^\infty \frac{\tilde{r}^{M-1} e^{-\frac{\tilde{r}}{2}}}{2^M \Gamma(M)} \prod_{b=1}^B \int_{r_b=0}^\infty \frac{1}{2} e^{-\frac{r_b}{2}} \left[1 - Q_1\left(\sqrt{\frac{\mu^2 r_b}{1-\mu^2}}, \sqrt{\frac{\tilde{\gamma}}{y}}\right)\right]^{L_b} \\
 &\quad \times \frac{1}{2} \left(\frac{y(1-\mu^2)}{\mu^2 \tilde{r}}\right)^{\frac{M-1}{2}} \exp\left(-\frac{y + \frac{\mu^2}{1-\mu^2} \tilde{r}}{2}\right) I_{M-1}\left(\sqrt{\frac{\mu^2 \tilde{r} y}{1-\mu^2}}\right) dr_b d\tilde{r} dy \\
 &\stackrel{(b)}{=} \left(\frac{1-\mu^2}{\mu^2}\right)^{\frac{M-1}{2}} \frac{1}{\Gamma(M)} \int_{y=0}^\infty \exp(-y) y^{\frac{M-1}{2}} dy \int_{\tilde{r}=0}^\infty \tilde{r}^{\frac{M-1}{2}} \exp\left(-\frac{\tilde{r}}{1-\mu^2}\right) I_{M-1}\left(2\sqrt{\frac{\mu^2 \tilde{r} y}{1-\mu^2}}\right) d\tilde{r} \\
 &\quad \times \prod_{b=1}^B \int_{r_b=0}^\infty e^{-r_b} \left[1 - Q_1\left(\sqrt{\frac{2\mu^2 r_b}{1-\mu^2}}, \sqrt{\frac{\tilde{\gamma}}{2y}}\right)\right]^{L_b} dr_b
 \end{aligned} \tag{G.4}$$

Therefore, the uplink WDT outage probability is bounded as

$$\begin{aligned}
 P_{\text{USPS}}^{\text{U}}(\hat{\gamma}) &> \int_0^\infty \dots \int_0^\infty F_{\beta_n|\alpha_n}\left(\frac{\hat{\gamma}}{y_1}, \dots, \frac{\hat{\gamma}}{y_B}\right) \\
 &\quad \times f_{\alpha_n}(y_1, \dots, y_B) dy_1 \dots dy_B. \tag{H.3}
 \end{aligned}$$

Finally, Eq. (59) is obtained by using the results of Eq. (H.1), Eq. (H.2), and Eq. (3.471.9) in [31] as well as some simplifications, which completes the proof.

## REFERENCES

- [1] J. Hu, K. Yang, G. Wen, and L. Hanzo, "Integrated data and energy communication network: A comprehensive survey," *IEEE Commun. Surveys Tuts*, vol. 20, no. 4, pp. 3169–3219, 2018.
- [2] X. Zhou, R. Zhang, and C. K. Ho, "Wireless information and power transfer in multiuser OFDM systems," *IEEE Trans. Wireless Commun.*, vol. 13, no. 4, pp. 2282–2294, 2014.
- [3] C. Psomas, K. Ntougias, N. Shanin, D. Xu, K. Mayer, N. M. Tran, L. Cottatellucci, K. W. Choi, D. I. Kim, R. Schober, and I. Krikididis, "Wireless information and energy transfer in the era of 6G communications," *Proc. IEEE*, pp. 1–41, 2024.
- [4] S. Bi, C. K. Ho, and R. Zhang, "Wireless powered communication: opportunities and challenges," *IEEE Commun. Mag.*, vol. 53, no. 4, pp. 117–125, 2015.
- [5] K.-K. Wong, A. Shojaefard, K.-F. Tong, and Y. Zhang, "Fluid antenna systems," *IEEE Trans. Wireless Commun.*, vol. 20, no. 3, pp. 1950–1962, 2021.
- [6] K.-K. Wong and K.-F. Tong, "Fluid antenna multiple access," *IEEE Trans. Wireless Commun.*, vol. 21, no. 7, pp. 4801–4815, 2022.
- [7] K.-K. Wong, D. Morales-Jimenez, K.-F. Tong, and C.-B. Chae, "Slow fluid antenna multiple access," *IEEE Trans. Commun.*, vol. 71, no. 5, pp. 2831–2846, 2023.
- [8] R. Zhang and C. K. Ho, "MIMO broadcasting for simultaneous wireless information and power transfer," *IEEE Trans. Wireless Commun.*, vol. 12, no. 5, pp. 1989–2001, 2013.
- [9] L. Tang, X. Zhang, P. Zhu, and X. Wang, "Wireless information and energy transfer in fading relay channels," *IEEE J. Sel. Areas Commun.*, vol. 34, no. 12, pp. 3632–3645, 2016.
- [10] R. R. Kurup and A. V. Babu, "Power adaptation for improving the performance of time switching SWIPT-based full-duplex cooperative NOMA network," *IEEE Commun. Lett.*, vol. 24, no. 12, pp. 2956–2960, 2020.
- [11] J. Park and B. Clerckx, "Joint wireless information and energy transfer in a  $k$ -user MIMO interference channel," *IEEE Trans. Wireless Commun.*, vol. 13, no. 10, pp. 5781–5796, 2014.
- [12] I. Budhiraja, N. Kumar, S. Tyagi, S. Tanwar, and Z. Han, "An energy efficient scheme for WPCN-NOMA based device-to-device communication," *IEEE Trans. Veh. Technol.*, vol. 70, no. 11, pp. 11935–11948, 2021.
- [13] H. Ju and R. Zhang, "Throughput maximization in wireless powered communication networks," *IEEE Trans. Wireless Commun.*, vol. 13, no. 1, pp. 418–428, 2014.
- [14] E. Boshkovska, D. W. K. Ng, N. Zlatanov, A. Koelpin, and R. Schober, "Robust resource allocation for MIMO wireless powered communication networks based on a non-linear EH model," *IEEE Trans. Commun.*, vol. 65, no. 5, pp. 1984–1999, 2017.
- [15] H. Pan, Y. Liu, G. Sun, J. Fan, S. Liang, and C. Yuen, "Joint power and 3D trajectory optimization for UAV-enabled wireless powered communication networks with obstacles," *IEEE Trans. Commun.*, vol. 71, no. 4, pp. 2364–2380, 2023.
- [16] C. Luo, J. Hu, L. Xiang, and K. Yang, "Reconfigurable intelligent sensing surface aided wireless powered communication networks: A sensing-then-reflecting approach," *IEEE Trans. Commun.*, vol. 72, no. 3, pp. 1835–1848, 2024.
- [17] Y. H. Al-Badarneh, C. N. Georghiades, and M.-S. Alouini, "Asymptotic performance analysis of the  $k$ -th best link selection over wireless fading channels: An extreme value theory approach," *IEEE Trans. Veh. Technol.*, vol. 67, no. 7, pp. 6652–6657, 2018.
- [18] R. Jiang, K. Xiong, P. Fan, L. Zhou, and Z. Zhong, "Outage probability and throughput of multirelay SWIPT-WPCN networks with nonlinear EH model and imperfect CSI," *IEEE Syst. J.*, vol. 14, no. 1, pp. 1206–1217, 2020.
- [19] W. K. New, K.-K. Wong, H. Xu, K.-F. Tong, and C.-B. Chae, "Fluid antenna system: New insights on outage probability and diversity gain," *IEEE Trans. Wireless Commun.*, vol. 23, no. 1, pp. 128–140, 2024.
- [20] —, "An information-theoretic characterization of MIMO-FAS: Optimization, diversity-multiplexing tradeoff and  $q$ -outage capacity," *IEEE Trans. Wireless Commun.*, vol. 23, no. 6, pp. 5541–5556, 2024.
- [21] K.-K. Wong, K.-F. Tong, Y. Chen, Y. Zhang, and C.-B. Chae, "Opportunistic fluid antenna multiple access," *IEEE Trans. Wireless Commun.*, vol. 22, no. 11, pp. 7819–7833, 2023.
- [22] H. Xu, K.-K. Wong, W. K. New, K.-F. Tong, Y. Zhang, and C.-B. Chae, "Revisiting outage probability analysis for two-user fluid antenna multiple access system," *IEEE Trans. Wireless Commun.*, vol. 23, no. 8, pp. 9534–9548, 2024.
- [23] X. Lin, H. Yang, Y. Zhao, J. Hu, and K.-K. Wong, "Performance analysis of integrated data and energy transfer assisted by fluid antenna systems," in *ICC 2024 - IEEE Int. Conf. Commun.*, 2024, pp. 2761–2766.
- [24] X. Lin, Y. Zhao, H. Yang, J. Hu, and K.-K. Wong, "Fluid antenna multiple access assisted integrated data and energy transfer: Outage and multiplexing gain analysis," *arXiv preprint arXiv:2407.10548*, 2024. [Online]. Available: <https://arxiv.org/abs/2407.10548>
- [25] C. Skouroumounis and I. Krikididis, "Simultaneous information and energy transfer in large-scale FA-enabled cellular networks," in *ICC 2024 - IEEE Int. Conf. Commun.*, 2024, pp. 4137–4142.

- [26] L. Zhang, H. Yang, Y. Zhao, and J. Hu, "Joint port selection and beamforming design for fluid antenna assisted integrated data and energy transfer," *IEEE Wireless Commun. Lett.*, vol. 13, no. 7, pp. 1833–1837, 2024.
- [27] X. Lai, K. Zhi, W. Li, T. Wu, C. Pan, and M. ElKashlan, "FAS-assisted wireless powered communication systems," in *2024 IEEE Int. Conf. Commun. (ICC Workshops)*, 2024, pp. 1731–1736.
- [28] F. R. Ghadi, M. Kaveh, K.-K. Wong, R. Jantti, and Z. Yan, "On performance of FAS-aided wireless powered NOMA communication systems," 2024. [Online]. Available: <https://arxiv.org/abs/2405.11520>
- [29] M. Khammassi, A. Kammoun, and M.-S. Alouini, "A new analytical approximation of the fluid antenna system channel," *IEEE Trans. Wireless Commun.*, vol. 22, no. 12, pp. 8843–8858, 2023.
- [30] P. Ramírez-Espinosa, D. Morales-Jimenez, and K.-K. Wong, "A new spatial block-correlation model for fluid antenna systems," *IEEE Trans. Wireless Commun.*, vol. 23, no. 11, pp. 15 829–15 843, 2024.
- [31] I. S. Gradshteyn and I. M. Ryzhik, *Table of integrals, series, and products*. Academic press, 2014.
- [32] H. Alzer, "On some inequalities for the incomplete gamma function," *Mathematics of Computation*, vol. 66, no. 218, pp. 771–778, 1997.
- [33] P. C. Sofotasios, S. Muhaidat, G. K. Karagiannidis, and B. S. Sharif, "Solutions to integrals involving the marcum  $Q$ -function and applications," *IEEE Signal Process. Lett.*, vol. 22, no. 10, pp. 1752–1756, 2015.
- [34] M. Abramowitz and I. A. Stegun, *Handbook of mathematical functions with formulas, graphs, and mathematical tables*. US Government printing office, 1968, vol. 55.